ACS OMEGA

http://pubs.acs.org/journal/acsodf

Article

Nafion Composite Membranes Impregnated with Polydopamine and Poly(Sulfonated Dopamine) for High-Performance Proton Exchange Membranes

T. S. Mayadevi, Bon-Hyuk Goo, Sae Yane Paek, Ook Choi, Youngkwang Kim, Oh Joong Kwon, So Young Lee, Hyoung-Juhn Kim, and Tae-Hyun Kim*

Cite This: *ACS Omega* 2022, 7, 12956−12970

Read Online

ACCESS | Metrics & More | Article Recommendations | Supporting Information

ABSTRACT: We prepared Nafion composite membranes by impregnating Nafion-212 with polydopamine, poly(sulfonated dopamine), and poly(dopamine-*co*-sulfonated dopamine) using the swelling−filling method to generate nanopores in the Nafion framework that were filled with these polymers. Compared to the pristine Nafion-212 membrane, these composite membranes showed improved thermal and mechanical stabilities due to the strong interactions between the catecholamine of the polydopamine derivatives and the Nafion matrix. For the composite membrane filled with poly(sulfonated dopamine) (N-PSDA), further interactions were induced between the Nafion and the sulfonic acid side chain, resulting in enhanced water uptake and ion conductivity. In addition, filling the nanopores in the Nafion matrix with polymer fillers containing aromatic hydrocarbon-based dopamine units led to an increase in the degree of crystallinity and resulted in a significant decrease in the hydrogen permeability of the composite membranes compared to Nafion-212. Hydrogen crossovers 26.8% lower than Nafion-212 at 95% relative humidity (RH) (fuel cell operating conditions) and 27.3% lower at 100% RH (water electrolysis operating conditions) were obtained. When applied to proton exchange membrane-based fuel cells, N-PSDA exhibited a peak power density of 966 mW cm^{-2}, whereas N-PSDA showed a current density of 4785 mA cm^{-2}, which is 12.4% higher than Nafion-212 at 2.0 V and 80 °C.

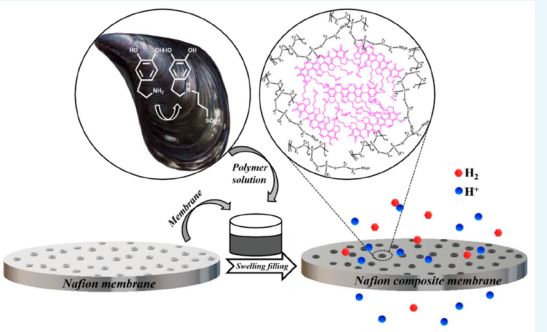

1. INTRODUCTION

A fuel cell is an energy conversion device that generates electricity using hydrogen as fuel. This technology is considered an eco-friendly energy source because it generates only water as a byproduct. Fuel cells are categorized into various types according to the electrolyte used. Proton exchange membrane-based fuel cells (PEMFCs) are currently widely employed in a range of applications, such as energy sources for transportation and power generation systems suitable for various areas because they provide high energy efficiency of about 45% and can operate under relatively low-temperature conditions from 60 to 80 °C.[1−3]

Meanwhile, hydrogen used as fuel for fuel cells is primarily obtained from byproducts generated in petrochemical processes, and carbon dioxide is inevitably generated during hydrogen production. As such, it is difficult to consider this energy source as completely eco-friendly. In contrast, water electrolysis is among the most eco-friendly hydrogen production methods because the technology generates hydrogen with zero carbon dioxide emission. Among the water electrolysis methods, proton exchange membrane-based water electrolysis (PEMWE) uses a proton exchange membrane (PEM) as an electrolyte; thus, the technology ensures high energy efficiency with no risk of electrolyte leakage. PEMWE systems also can operate under high voltage conditions and can be implemented in a compact design. For these reasons, this technology has been attracting significant attention.[4−6]

A PEM is a key component of PEMFC and PEMWE systems that allows protons to be conducted between the anode and cathode and separates the two electrodes from each other. These PEMs significantly affect the overall performance of fuel cells and water electrolyzers. Therefore, a great deal of research has addressed developing PEM materials that provide not only high ionic conductivity but also excellent physicochemical stability.

Among commercially available PEM materials, Nafion consists of a perfluoroalkyl-based main chain and side chains containing sulfonic acid groups. Due to its unique structure,

Received: January 13, 2022
Accepted: March 25, 2022
Published: April 6, 2022

https://doi.org/10.1021/acsomega.2c00263
ACS Omega 2022, 7, 12956−12970

this polymeric material exhibits a distinct phase separation between the hydrophobic and hydrophilic domains. Thus, Nafion-based membranes provide both excellent mechanical properties and electrochemical stability. The sulfonic acid groups contained in these membranes tend to gather, forming a unique fringed-rod-like morphology. Nafion-based membranes provide high ionic conductivity and excellent stability due to this unique morphology.[7−9]

However, the proton conductivity of Nafion and other perfluorosulfonic acid (PFSA)-based polymer membranes depends on relative humidity (RH); thus, achieving high ionic conductivity requires that a highly hydrated condition be maintained. In a humidified or hydrated state, however, water serves as a plasticizer, lowering the glass-transition temperature, T_g, of polymers. This leads to a change in the morphology of Nafion in the actual operating conditions of cells, thereby degrading their mechanical properties while abruptly accelerating hydrogen permeability.[9,10] The occurrence of this hydrogen crossover results in enhanced Ohmic potential and reduced current density under the actual operating conditions of cells. This directly not only lowers fuel cell performance (for PEMFC) and hydrogen production efficiency (for PEMWE) but also leads to the formation of hydrogen peroxides and hydroperoxyl radicals that negatively affect the long-term duration of the PEMs.[7,11]

Much research has been conducted to ensure that Nafion can maintain its high ionic conductivity and excellent physicochemical stability even under high-temperature and humidified conditions. These studies have focused mainly on composite materials in which Nafion dispersion solutions are blended with inorganic materials, such as composite membranes made of sulfonated silica and Nafion,[12] Nafion composite membranes blended with sulfonated graphene oxides,[13] and composite membranes made of carbon nanotubes containing amine-functionalized cerium oxides and Nafion.[14] Most of these studies successfully achieved the intended conductivity improvement compared to typical Nafion membranes, but information about hydrogen crossover was not reported.

Meanwhile, sulfonated aromatic hydrocarbon has attracted wide attention as an alternative PEM material for Nafion.[15−18] Some attempts have been made to overcome the limitations of Nafion-based membranes by mixing this material with Nafion. For example, various composite membranes were developed by combining sulfonated poly(arylene ether ketone) (sPAEK) with Nafion.[19] Composite membranes fabricated using these approaches showed improved ionic conductivity and mechanical and oxidative properties compared to typical Nafion membranes. However, due to poor compatibility between Nafion and the applied additives, the overall performance of membranes was degraded. However, these approaches are somewhat effective in reducing methanol crossover in direct methanol fuel cells (DMFCs), where methanol is used as a fuel.[19]

Recently, a swelling−filling (SF) method was developed for minimizing the occurrence of phase separation between heterogeneous polymers during the fabrication of Nafion composite membrane.[20−25] In this method, Nafion membranes are subjected to swelling by organic solvents to maximize the pore size, and additives are then added to fill these pores. Proton conductive macromolecules (PCMs) with nanospherical morphology are used as additives to fill nanopores while further facilitating the interaction between the sulfonic acid groups of Nafion and the hydrophilic functional groups of the additives in the swollen Nafion framework. Nafion composite membranes fabricated by this swelling−filling method may have a nanophase-separated morphology, unlike existing composite membranes with a macrophase-separated morphology. With these unique structural features, these membranes provide improved ionic conductivity and physical and chemical stability. Some studies on SF composite membranes have introduced sheared graphene oxides or nano-sized functionalized silica into Nafion and other types of SF composite membranes.[23] These methods were also somewhat effective in reducing the crossover of methanol as a fuel, but little research has been conducted on hydrogen permeability.

Meanwhile, due to the catechol and amine functional groups contained in its structure, polydopamine, which is derived from mussels (and mimicks the adhesive strength of mussels), is known to have strong adhesion to the surface of a wide range of materials, such as poly(tetrafluoroethylene) (PTFE), metals, nonmetals, organic polymers, and inorganic materials.[26−28] Because its strong adhesion forces allow it to be coated on almost all kinds of surfaces, polydopamine is currently widely used in various surface modification applications. For example, this material has been used in the electroless deposition process of metallic silver and gold, as an organic electrode material in energy storage devices for lithium and sodium batteries,[26] and recently as a coating material for PTFEs along with cerium oxides (CeO_x) in PEM applications.[29]

Polydopamine is generated via the spontaneous oxidation of dopamine.[30] This material is characterized by containing low-molecular-weight dopamine species capable of penetrating the three-dimensional porous surface of a material with nano-sized pores and then adsorbing onto the surface. In a recent study, polydopamine and a PFSA dispersion agent were blended; the resultant composite membranes provided improved mechanical properties and reduced hydrogen permeability.[31] This was attributed to the $\pi-\pi$ stacking of dopamine molecules enhancing the physical stability of the composite membranes, as well as a number of hydrophilic groups contained in the dopamine structure that also induced hydrogen bonds and electrostatic mutual attraction. Further, it has recently been reported that polydopamine itself can conduct protons.[32]

In the present study, both dopamine and sulfonated dopamine were polymerized to form polydopamine and poly(sulfonated dopamine), and the sulfonated dopamine was also copolymerized with dopamine to obtain poly(dopamine-*co*-sulfonated dopamine). Subsequently, the obtained materials were introduced as additives to fabricate Nafion composite membranes impregnated with these polymers using the SF method. These novel PEM materials were examined for their applicability to PEMFCs and PEMWEs. As described earlier, the swollen pores of Nafion membranes were effectively filled with poly(sulfonated dopamine) or poly(dopamine-*co*-sulfonated dopamine) via the SF method, allowing the resultant composite membranes to have a nanophase-separated morphology. As a result, improved conductivity and physicochemical properties are expected, together with reduced hydrogen crossover. The physicochemical and electrical properties of the obtained composite membranes, along with the properties of PEMFCs and PEMWE cells using the membranes, were examined, and the results were compared to those obtained from pristine Nafion-212 and polydopamine-filled Nafion composite mem-

https://doi.org/10.1021/acsomega.2c00263
ACS Omega 2022, 7, 12956−12970

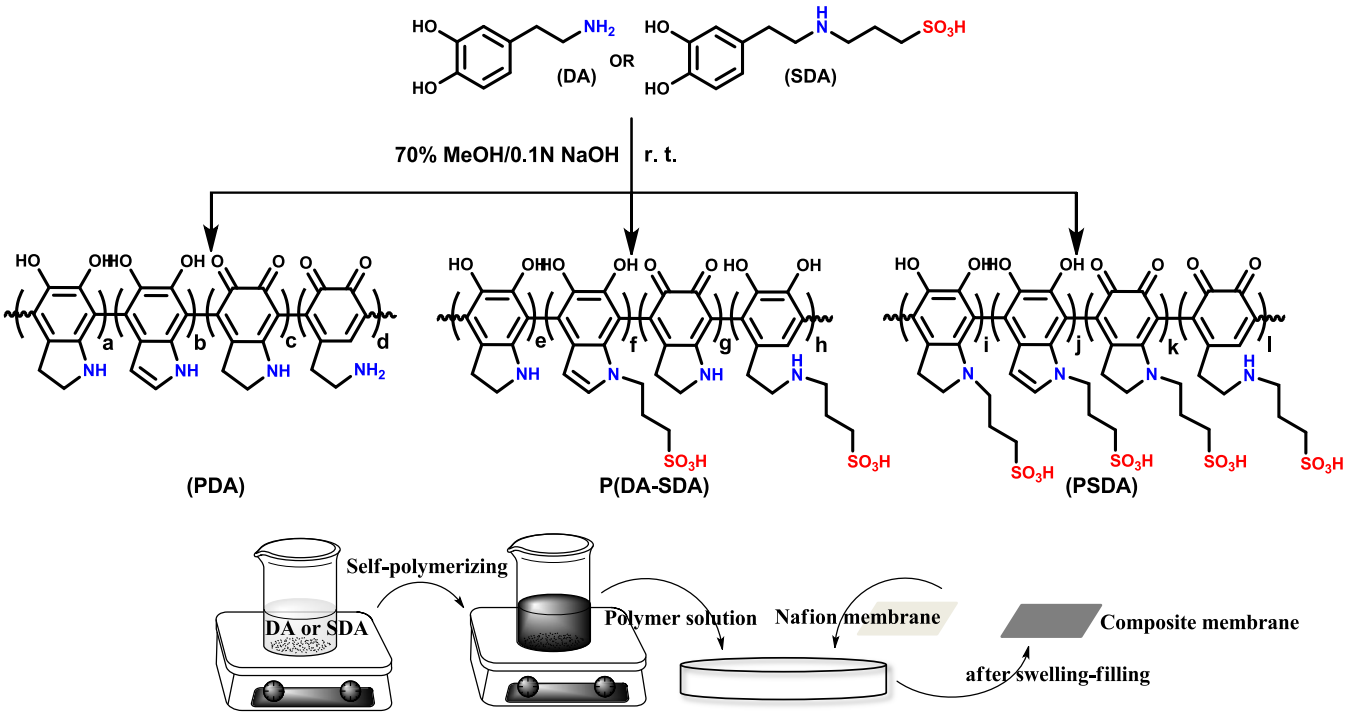

Figure 1. Schematic representation of the synthesis of three different types of dopamine homopolymer and copolymers using DA and SDA, and the preparation of Nafion composite membranes using these polymers through the swelling−filling method.

branes. To our knowledge, this is the first example of using polydopamine or functionalized polydopamine as an impregnation agent to Nafion.

2. EXPERIMENTAL SECTION

2.1. Materials. Dopamine hydrochloride was purchased from Sigma-Aldrich (Yongin, Korea). 1,3-Propane sultone was obtained from Tokyo Chemical Industries Ltd. (Seoul, Korea). Nafion-212 membrane was available from a local vendor. All other chemicals and solvents, such as NaOH, HCl, ammonia solution, and methanol, were purchased from Daejung Metals & Chemicals Co., Ltd. (Shiheung, Korea) and used as received. Deionized (DI) water was used throughout this study for membrane treatment and measuring properties.

2.2. Synthesis of Sulfonated Dopamine (SDA). The sulfonated dopamine (SDA) was prepared following the procedures reported as follows.[33] First, 2.27 g of dopamine hydrochloride (DA) was dissolved in 300 mL of anhydrous ethanol to form a homogeneous solution in a round-bottom flask. Afterward, 1.6 g of 1,3-propane sultone and 0.832 mL of ammonia solution were successively added into the DA/ethanol solution. The resulting solution was heated at 50 °C for 18 h. The final SDA (yield of 40%) was obtained by filtration from the final solution and washing in ethanol several times, followed by drying at 40 °C in an oven for 24 h to give the product as a white solid; δ_H (400 MHz, D_2O) 6.86 (1H, d, J = 8.0, H_2), 6.80 (1H, s, H_3), 6.71 (1H, d, J = 8.0, H_1), 3.25 (2H, t, J = 8.0, H_8), 3.16 (2H, t, J = 8.0, H_5), 2.95 (2H, t, J = 8.0, H_6), 2.86 (2H, t, J = 8.0, H_4), 2.07 (2H, p, J = 8.0, H_7).

2.3. Preparation of the Polydopamine Derivatives. Each polydopamine-derivative solution was prepared by modifying the reported procedure. First, polydopamine (PDA), poly(dopamine-*co*-sulfonated dopamine) [P(DA-SDA)], and poly(sulfonated dopamine) (PSDA)were prepared by the oxidative polymerization using their corresponding monomers (Figure 1)[34] as follows:

For the preparation of PDA, 0.25 g of dopamine (DA) was completely dissolved in 42 mL of 70% MeOH (MeOH/H_2O = 7:3) with a concentration of 0.6 wt %, followed by adding a few drops of 0.1 N NaOH and stirring at room temperature. The reaction was carried out until the appearance of the solution changed from colorless to dark brown or black, indicating complete polymerization.

For P(DA-SDA), 0.125 g of DA and 0.125 g of SDA (1:1 ratio by weight) were combined using the same procedure as above. The PSDA polymer solution was also prepared in the same way, using 0.25 g of SDA. All of these polymer solutions were used for filling the Nafion membrane to produce the corresponding composite membranes.

2.4. Preparation of Composite Polymer Membranes. Each Nafion composite membrane was directly filled with the polydopamine-derivative solutions as follows: each polymer solution (42 mL in 70% MeOH) was prepared in a vial. Subsequently, the Nafion membrane was placed in the prepared PDA, P(DA-SDA), and PSDA solutions for 36 h to yield N-PDA, N-P(DA-SDA), and N-PSDA membranes, respectively. Afterward, the solvent was removed by heating the treated membranes at 70 °C for 24 h. In addition, a pristine Nafion membrane treated in 70% MeOH was also prepared (N-MeOH) using the method mentioned above along with Nafion-212 membrane as a reference. All polymer-filled composite membranes had thicknesses in the range of 50−60 μm. Next, all of the membranes were acidified with 1M HCl at 50 °C for 5 h, then washed with deionized (DI) water at least three times.

2.5. Characterization and Measurement Methods. All characterization and measurement methods are described in detail in the Supporting Information.

https://doi.org/10.1021/acsomega.2c00263
ACS Omega 2022, 7, 12956−12970

3. RESULTS AND DISCUSSION

3.1. Synthesis and Characterization of Polydopamine, Poly(Sulfonated Dopamine), and Poly(Dopamine-*co*-Sulfonated Dopamine). First, dopamine and 1,3-propane sultone were allowed to react in an ammonia solution to obtain sulfonated dopamine (SDA) (Scheme S2).

The synthesized sulfonated dopamine (SDA) was then subjected to structural analysis by comparing it with dopamine (DA) as a reference through a comparative spectroscopic analysis using proton nuclear magnetic resonance (^{1}H NMR) and Fourier transform infrared (FT IR) (Figure S1). In the ^{1}H NMR spectrum of DA, peaks corresponding to aromatic protons ($H_{1,2,3}$) and alkyl protons ($H_{4,5}$) were observed at 6.70−6.87 ppm and 2.80−3.20 ppm, respectively. In the spectrum of SDA, however, new peaks appeared at 2.07 (H_7), 2.95 (H_6), and 3.25 (H_8) ppm in addition to the peaks mentioned above. The newly introduced peaks were attributed to propyl sulfonates (Figure S1a).

The structure of SDA was further confirmed using the FT IR spectroscopic analysis, where a new absorption peak corresponding to the S═O stretching of SO_3 was observed at 1056 cm^{-1}. These results confirmed the successful synthesis of SDA (Figure S1b).

Next, dopamine and sulfonated dopamine were used to synthesize the following three polymers: dopamine homopolymer (polydopamine, PDA), sulfonated dopamine homopolymer [poly(sulfonated dopamine), PSDA], and dopamine-sulfonated dopamine copolymer [poly(dopamine-*co*-sulfonated dopamine), P(DA-SDA)]. Each polymerization process was conducted in basic conditions: a 0.6 wt % MeOH solution ($MeOH/H_2O$ = 7:3) (Figure 1).

During this reaction, 5,6-dihydroxyindole (DHI) is formed as a reaction intermediate via nucleophilic cyclization between dopamine molecules, followed by polymerization through autoxidation between these molecules. The hydroxide ions in the reaction solution are known to facilitate the rate-determining step (r.d.s.), thereby accelerating the formation of nanoparticle-type polydopamine.[26] In the synthesis of P(DA-SDA), DA and SDA were mixed in a weight ratio of 1:1.

With the formation of polydopamine via the oxidation of dopamine, the corresponding solutions were found to gradually turn black. In the polymerization process using DA, the corresponding solutions quickly turned dark brown due to their high reactivity for polymerization. However, the color change was very slow in the polymerization process using SDA (i.e., the fabrication of P(DA-SDA) and PSDA) because the polymerization of the relevant monomers was slowed by the electrostatic repulsion of the sulfonate groups.[33] The polymerization process was conducted for at least 5 days, given the difference in the reactivity of monomers. It was found that, after that period, all solutions turned dark black (Figure S2).

The polymerization of the three types of dopamine and their derivatives was confirmed based on the UV−vis spectra. The formation of polydopamine allowed each molecular component to have a conjugation structure in the form of quinone.[33,35−37] As a result, a shoulder absorption peak was observed at ∼350 nm in all three polymers, which indicated the successful synthesis of the intended polymers (Figure S3).

In addition, an energy-dispersive X-ray spectroscopy (EDS) mapping analysis was conducted on the three fabricated dopamine (DA)-based polymer particles using SEM (Figure S4 and Table S1). The quantitative elemental analysis results showed sulfur content of 3.03% in P(DA-SDA) and 5.25% in PSDA. This confirmed that sulfonated dopamine had participated in the polymerization process.

FT IR spectroscopic analysis was conducted for further structural analysis of the obtained polymers (Figure S5). Characteristic peaks corresponding to the C═O bonds from quinone were observed at 1610 cm^{-1} in all three polymers.[38,39] In addition, an adsorption band, corresponding to the stretching vibration of NH groups (at 1521 cm^{-1}), a peak corresponding to the vibration of methylene C−H (at 1470 cm^{-1}), a peak corresponding to the vibration of phenolic C−O−H bonds (at 1390 cm^{-1}), and a peak corresponding to C−O bonds (at 1285 cm^{-1}) were observed. In P(DA-SDA) and PSDA, in particular, a peak corresponding to the symmetric stretching vibration of SO_3 groups was additionally observed at 1041 cm^{-1}.[31,39−41] These results confirmed the successful oxidative self-polymerization of DA, SDA, and DA-SDA in alkaline solutions.

3.2. Fabrication and Characterization of Nafion Composite Membranes Filled with PDA Derivatives. The three polymer solutions (PDA, PSDA, and P(DA-SDA)) were used to fabricate Nafion composite membranes according to the following procedures (Figure 1). First, Nafion-212 membranes were immersed in aqueous MeOH solutions (0.6 wt %) of PDA, PSDA, and P(DA-SDA) for 36 h and then dried. In the process, these Nafion membranes were subjected to swelling by MeOH as a solvent; at the same time, the newly developed micropore structure of Nafion was impregnated with the polymers in situ.

These Nafion composite membranes, impregnated with three different polymers: polydopamine, poly(dopamine-*co*-sulfonated dopamine), and poly(sulfonated dopamine), were obtained in the form of a flexible film; these films were, respectively, denoted as N-PDA, N-P(DA-SDA), and N-PSDA (Figure S6). In addition, a Nafion membrane was subjected to swelling by methanol without the addition of polymers as impregnation agents to fabricate a Nafion composite membrane filled with methanol. This membrane was then named N-MeOH and used to compare the changes in some basic membrane properties of the pristine Nafion-212 control group (Figure S6).

The structural analysis of the Nafion composite membranes filled with the polydopamine derivatives, that is, N-PDA, N-P(DA-SDA), and N-PSDA, was performed via FT IR, and the results were compared to those obtained from Nafion-212 as a control group (Figure S7). Absorption bands characteristic of Nafion-based polymers were observed in all tested materials. More specifically, peaks corresponding to the stretching vibration of fluorocarbon chains appeared at 1201 and 968 cm^{-1}, and peaks corresponding to the symmetric and asymmetric stretching vibration of O═S═O in the $-SO_3H$ groups were observed at 1140 and 1056 cm^{-1}.

The introduction of different fillers (PDA, P(DA-SDA), and PSDA) into the Nafion matrix caused the intensity of the peak corresponding to the O═S═O vibration to decrease. This was attributed to the electrostatic attraction generated at the interface between the SO_3H groups of the Nafion matrix and the functionalized polymer fillers. To be more specific, this attraction corresponded to the interaction between the SO_3H groups in the matrix and the hydroxyl groups or amine groups contained in the dopamine molecules (−S═O···H−O− and −S═O···H−N−). Some absorption bands appeared in the composite membranes that were not observed in Nafion-212.

https://doi.org/10.1021/acsomega.2c00263
ACS Omega 2022, 7, 12956−12970

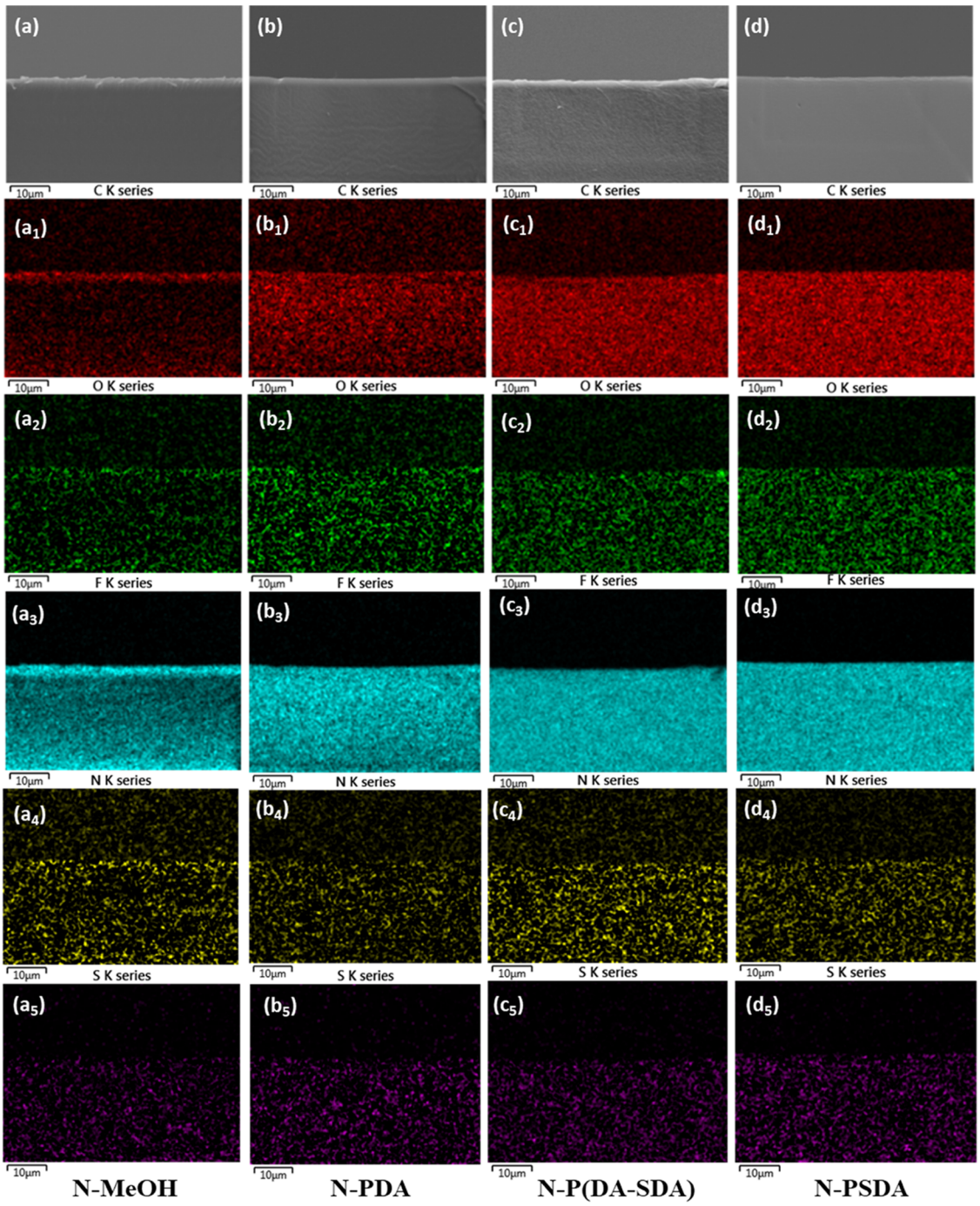

Figure 2. SEM cross-sectional images of the pretreated membranes: (a–d) secondary electron images, (a_1–d_1) EDS mapping images with carbon (C) elemental maps, (a_2–d_2) EDS mapping images with oxygen (O) elemental maps, (a_3–d_3) EDS mapping images with fluorine (F) elemental maps, (a_4–d_4) EDS mapping images with nitrogen (N) elemental maps, and (a_5–d_5) EDS mapping images with sulfur (S) elemental maps: N-MeOH (a series), N-PDA (b series), N-P(DA-SDA) (c series), and N-PSDA (d series).

These new absorption bands appeared in the range of 2000–1300 cm^{-1}. More specifically, peaks corresponding to the indole or indoline structure, the stretching vibration of NH groups, the bending vibration of methylene C–H bonds, and phenolic C–O–H bonds were observed at 1610, 1521, 1470, and 1390 cm^{-1}, respectively (Figure S7b). These results confirmed that the three different polydopamine-derivative fillers had been successfully impregnated into the micropores of each Nafion membrane.

Next, the density of the three obtained Nafion composite membranes was measured, and the results were compared to those obtained from N-MeOH. These composite membranes were expected to have high-density networks because their internal pores were impregnated with the PDA-based fillers. The density of the membranes was examined with respect to the duration of the swelling–filling process to confirm this. The results showed that the density of N-MeOH remained constant regardless of the duration of the process, while the density of the composite membranes N-PDA, N-P(DA-SDA),

https://doi.org/10.1021/acsomega.2c00263
ACS Omega 2022, 7, 12956–12970

Table 1. IEC, Water Uptake, and Swelling Ratio of the Nafion-212, N-MeOH, N-PDA, N-P(DA-SDA), and N-PSDA Membranes

membrane	exp. IEC (meq g^{-1})	water uptake (%)		swelling ratio (%)			
		20 °C	80 °C	20 °C (Δl)	80 °C (Δl)	20 °C (Δt)	80 °C (Δt)
Nafion-212	0.91 ± 0.06	14.10 ± 0.27	32.90 ± 0.18	13.9 ± 0.17	20.9 ± 0.11	13.2 ± 0.25	23.0 ± 0.27
N-MeOH	0.92 ± 0.09	30.53 ± 0.17	47.20 ± 0.13	18.2 ± 0.50	29.5 ± 0.25	21.8 ± 0.32	30.8 ± 0.27
N-PDA	0.75 ± 0.01	24.18 ± 0.31	40.05 ± 0.12	13.6 ± 0.34	20.5 ± 0.20	12.5 ± 0.42	21.4 ± 0.18
N-P(DA-SDA)	0.78 ± 0.01	26.10 ± 0.24	43.41 ± 0.18	15.9 ± 0.29	22.7 ± 0.51	15.5 ± 0.37	24.1 ± 0.49
N-PSDA	0.83 ± 0.00	28.03 ± 0.13	45.71 ± 0.63	17.3 ± 0.19	23.2 ± 0.39	16.4 ± 0.26	25.5 ± 0.31

and N-PSDA increased over time (Table S2). The density changes were attributed to filling the micropores present inside these MeOH-treated Nafion membranes with the polymer fillers.

Once the duration of the swelling−filling process exceeded 36 h, no density change was observed in all membranes, which confirmed that the pores in the Nafion membranes had been completely filled with the polymer fillers. These membranes were then used for further analysis and characterization.

The densities of the fully impregnated composite membranes were then compared. The density of N-MeOH was lower than that of pristine Nafion-212 due to the swelling of the membrane after methanol treatment. The density decreased for the membranes in the following order: SDA [N-PDA (1.991) > N-P(DA-SDA) (1.934) ∼ N-PSDA (1.932)] because the introduction of SDA led to an increase in the free volume inside the membranes. More specifically, unlike dopamine, sulfonated dopamine contains flexible aliphatic chains that fill the Nafion micropores differently.

The fractional free volume (FFV) of the applied polydopamine derivatives was calculated to confirm this mechanism (Table S3). In general, polymers containing rigid side chains or bulky functional groups, such as sulfonated groups, are known to have relatively large FFVs. Indeed, the FFV of the polymer fillers was found to increase with increasing SDA content (PDA < P(DA-SDA) < PSDA). These FFV results confirmed that the degree of filling might be altered by the introduction of SDA; this was also consistent with the tendency observed in the membrane density measurements. Simply put, the introduction of SDA with relatively large FFV led to a decrease in the density of the membranes. The FFV is directly related to the amount of space that can be occupied by the water molecules contained in the applied polymer, and the conductivity of the resultant membranes can be further affected.

Subsequently, scanning electron microscopy (SEM) was conducted to characterize the surface and cross section of the three Nafion composite membranes [N-PDA, N-P(DA-SDA), and N-PSDA], and the results were compared to those obtained from N-MeOH (Figure S8). All three composite membranes were found to have a smooth, dense, and uniform surface. This uniform and homogeneous microstructure was attributed to the hydrophilic groups (amino, imino, and catechol groups) contained in the dopamine structure of the impregnation agents that induce additional interactions and form a physical interaction with the Nafion matrix.

Elemental analysis was also conducted on the cross section of the three Nafion composite membranes via energy-dispersive X-ray spectroscopy (EDS) mapping, and the results were compared to those obtained from N-MeOH (Figure 2 and Table S4). The cross section of all membranes was smooth and homogeneous, as in the SEM surface analysis results. The elemental analysis results showed that the carbon content was higher, and the fluorine content was lower in the composite membranes impregnated with the polymer fillers than in the N-MeOH control (with a carbon content of 37.70% and a fluorine content of 57.41%). This confirmed that dopamine, an aromatic hydrocarbon material, had been successfully impregnated into each Nafion membrane. The O/C content ratio increased in the order of N-PDA < N-P(DA-SDA) < N-PSDA because an increase in the SDA content of the impregnation agent led to an increase in the proportion of the sulfonic acid groups.

Overall, these SEM analysis results confirmed that no defects resulting from nonuniform phase separation between the Nafion matrix and the two polydopamine polymers were observed in the Nafion composite membranes. The polydopamine-derivative fillers were uniformly distributed throughout the Nafion matrix.

3.3. Ion Exchange Capacity (IEC), Water Uptake (WU), and Swelling Ratio (SR) of the Nafion Composite Membranes. The ion exchange capacity (IEC), water uptake (WU), and swelling ratio (SR) of the three Nafion composite membranes [N-PDA, N-P(DA-SDA), and N-PSDA] were analyzed, and the results were compared to those obtained from Nafion-212 and N-MeOH (Table 1).

The IEC refers to the milliequivalent of ion-conducting groups present in polymers and is closely related to the ionic conductivity and WU of membranes. In general, the higher the IEC of a membrane is, the higher its ionic conductivity becomes; however, this is likely to significantly increase the WU, leading to an excessive increase in the SR.

The IEC of the composite membranes was experimentally measured using acid−base titration (i.e., IEC_{exp}), and the results are presented in Table 1. The N-MeOH (0.92 meq g^{-1}) with no polymers added showed almost the same IEC_{exp} as that of Nafion-212 (0.9 meq g^{-1}) (Table 1). The figures for N-PDA, N-P(DA-SDA), and N-PSDA were then measured to be 0.75, 0.78, and 0.83 meq g^{-1}, respectively. Simply put, the three Nafion composite membranes impregnated with the polymers showed slightly lower IEC than Nafion-212 and N-MeOH as control groups. This indicates that introducing polymer fillers into a Nafion membrane leads to an increase in the total mass of the resultant composite membrane, thereby lowering its IEC_{exp}. N-PDA, in particular, exhibited the lowest IEC, and the IECs of N-P(DA-SDA) and N-PSDA were slightly higher than that of N-PDA. This was attributed to the sulfonic acid groups contained in SDA.

Next, the WU and SR of each composite membrane were measured and compared with Nafion-212 and N-MeOH. These two parameters are primary factors determining the physical and mechanical properties of membranes. The WU, in particular, closely affects not only the physical properties but also the ionic conductivity of PEMs because the presence of a

https://doi.org/10.1021/acsomega.2c00263
ACS Omega 2022, 7, 12956−12970

sufficient number of water molecules in the membrane leads to the formation of ion channels, which help promote the diffusion of protons while enhancing stability. However, excessively high WU inevitably degrades the dimensional stability of membranes, resulting in a decrease in their mechanical properties and the overall performance of the resultant membrane−electrode assembly (MEA). Not only that, the WU and SR of a membrane are known to depend on the porosity of the membrane; high porosity leads to a high WU and SR.[42−44]

The WU and SR values of each membrane measured at low (20 °C) and high (80 °C) temperatures are presented in Table 1. The results showed that both WU and SR were increased for N-MeOH compared to the pristine Nafion-212 because the methanol treatment caused the Nafion-212 membrane to swell. The composite membranes also exhibited higher WU and similar or slightly higher SR than Nafion-212. All of the composite membranes, however, showed lower WU and SR (i.e., higher dimensional stability) than the N-MeOH membrane. More specifically, N-MeOH showed the highest WU and SR (or lowest dimensional stability). The WU values of the polydopamine-filled Nafion (N-PDA) were 24.18 and 40.05% at 20 and 80 °C, respectively, lower than those of N-MeOH at 30.53 and 47.20% at 20 and 80 °C, respectively. This was attributed to the fact that N-PDA exhibited a lower IEC than N-MeOH and also to the fact that N-PDA was fabricated by filling the pores of a Nafion membrane with PDA-based fillers that are more aromatic and, thus, more hydrophobic in nature than Nafion.

At both 20 and 80 °C, the increasing content of PSDA led to an increase in the WU and SR (N-PDA < N-P(DA-SDA) < N-PSDA). This was attributed to the sulfonic acid groups present in the flexible side chains of the SDA units. In other words, the introduction of hydrophilic sulfonic acid groups helped attract more H_2O molecules. Here, note that the composite membranes impregnated with PSDA showed lower WU and SR at both low and high temperatures than N-MeOH even though all membranes had a similar IEC. These results were attributed to the strong interaction between Nafion and PSDA and between PSDAs, resulting in increased swelling and dimensional stability of the composite membranes.

3.4. Mechanical and Thermal Properties of the Membranes. Next, the stress−strain curves of the obtained composite membranes were measured at room temperature and 50% RH to examine their mechanical stability (Figure 3 and Table S5). The results showed that the tensile strength of Nafion-212 as a control group was 15.5 MPa, while its elongation at break was 277.7%. However, N-PDA, N-P(DA-SDA), and N-PSDA all exhibited similar or higher tensile strength than Nafion-212. This was because the composite membranes were fabricated by filling the pores of Nafion membranes with PDA-based fillers that are physically stable due to the $\pi-\pi$ stacking between catechol structures. In addition, various hydrophilic functional groups contained in the dopamine monomers (including amino, imino, and catechol groups) served to form hydrogen bonds and electrostatic interactions with the sulfonic acid functional groups of Nafion. Accordingly, the tensile strength tended to increase with increasing SDA content, that is, 15.0 MPa for N-PDA, 15.9 MPa for N-P(DA-SDA), and 17.6 MPa for N-PSDA. The elongation at break also increased with increasing SDA content, that is, 204.1% for N-PDA, 210.1% for N-P(DA-SDA), and 263.4% for N-PSDA. Overall, the Nafion composite

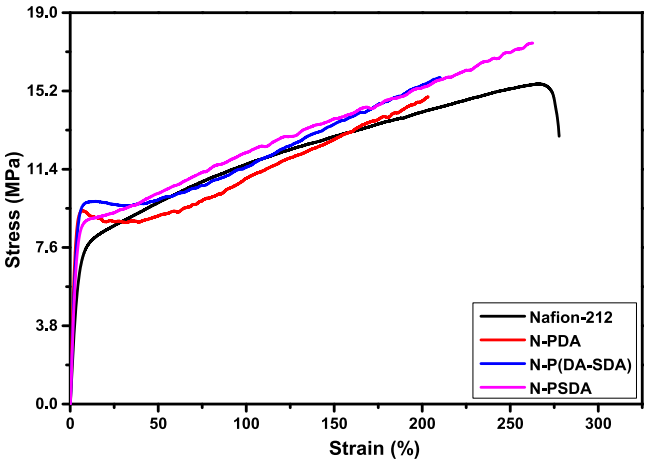

Figure 3. Stress−strain curves of the composite membranes with different polymer fillers and the reference membrane.

membranes filled with the dopamine-derivative fillers exhibited excellent mechanical performance with significantly higher tensile properties while still providing similar levels of elongation as Nafion-212.

Thermogravimetric analysis (TGA) was performed to examine the thermal degradation behavior of each membrane (Figure 4). All tested membranes exhibited the characteristic

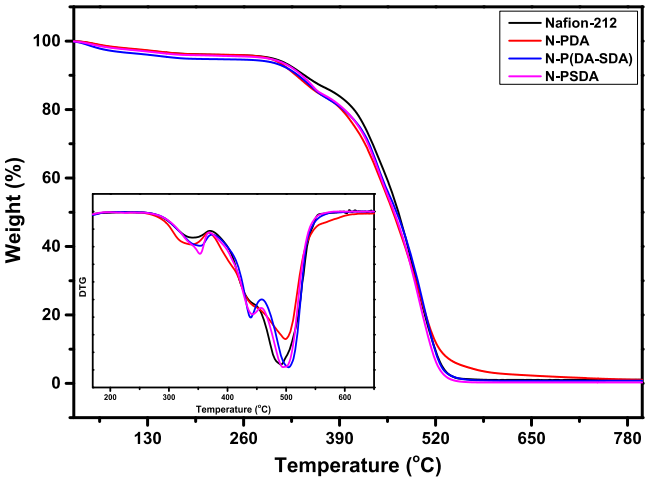

Figure 4. TGA curves from 30 to 800 °C were obtained from the reference and composite membranes (inset: DTG of the TGA thermograph).

thermal behavior of Nafion. More specifically, a weight loss was observed below 200 °C, which corresponded to the evaporation of the water and solvents contained in the membrane. The weight loss observed in the range of 280−400 °C was attributed to the degradation of the sulfonic acid groups present in the side chains of Nafion (and the sulfonic acid groups attached to the side chains of the PSDA units). In the range of 400−500 °C, a weight loss corresponding to the degradation of Nafion's side chains was observed. Above 500 °C, a weight loss resulting from the degradation of the PTFE backbone was detected. In N-P(DA-SDA) and N-PSDA, the maximum degradation temperatures of the sulfonic acid groups were 354 and 353 °C, respectively—slightly higher than that of N-PDA at 339 °C. This was attributed to the strong interaction between the functional groups inside the sulfonated dopamine

https://doi.org/10.1021/acsomega.2c00263
ACS Omega 2022, 7, 12956−12970

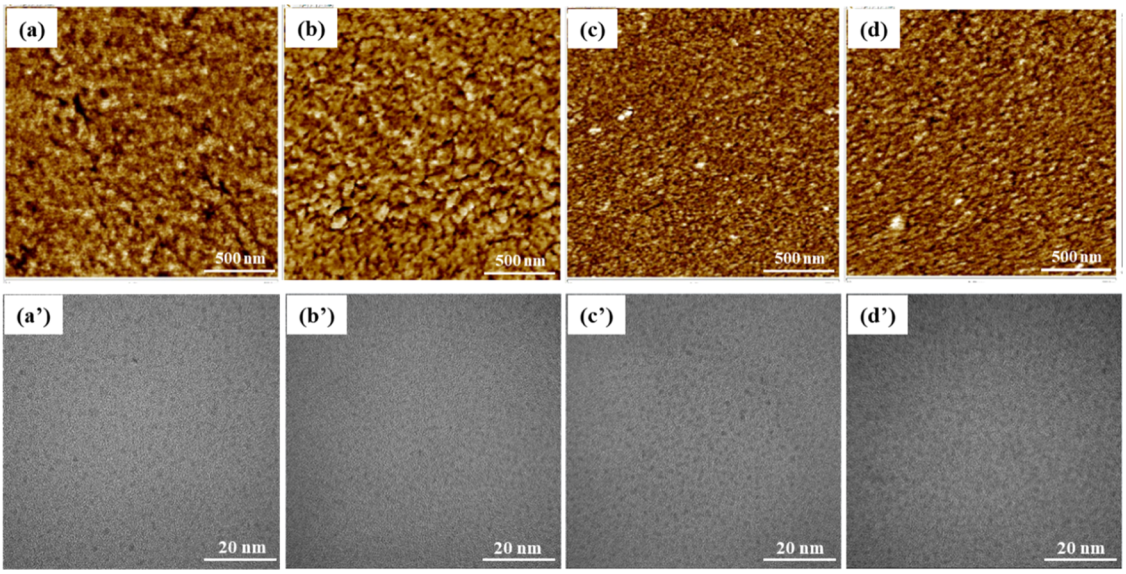

Figure 5. AFM phase images of (a) Nafion-212, (b) N-PDA, (c) N-P(DA-SDA), and (d) N-PSDA, and transmission electron microscopy (TEM) images of (a′) Nafion-212, (b′) N-PDA, (c′) N-P(DA-SDA), and (d′) N-PSDA.

(catecholamine) units. In N-P(DA-SDA) and N-PSDA, in particular, an additional weight loss corresponding to the degradation of the alkyl side chains of the SDA units was observed at around 440 °C in the side chain degradation temperature range of 400−500 °C. These results again confirmed that different amounts of SDA fillers had been impregnated into each Nafion membrane.

The thermal analysis can be further validated by DSC for all three composite membranes and pristine Nafion-212, and the obtained curves are presented in Figure S9. The relaxation process during the structural reorganization of polymer results in the appearance of endothermic peaks. The glass-transition temperatures (T_g) for each composite membrane were compared with Nafion-212 (Figure S9). The pristine Nafion-212 showed T_g at 83.4 °C, whereas N-PDA, N-P(DA-SDA), and N-PSDA showed a value at 78.2, 85.9, and 87.1 °C, respectively, indicating that T_g increased with the increase of SDA content. This is ascribed to the strong interaction between the sulfonic acid side chains in the PSDA unit and Nafion.

Overall, the Nafion-filling strategy using sulfonated dopamine-derivatives helped to improve the thermal properties of composite membranes compared to pristine Nafion-212.

A water state analysis of each composite membrane was further conducted using DSC and compared with that of Nafion-212 (Figure S10). In all tested membranes, depression of the freezing point for bound water was observed. This phenomenon can be interpreted as a peak shift to lower temperatures caused by loosely bound water. More specifically, it was attributed to the interaction between the sulfonic acid groups of Nafion and loosely bound water. However, in N-PSDA with the PSDA fillers, the degree of freezing point depression was greater than other membranes. This was attributed to the introduction of sulfonic acid groups from the SDA-containing fillers. Thus, N-PSDA exhibited improved water holding capacity and was also expected to provide improved ionic conductivity and cell performance accordingly.

3.5. Morphological Analysis. A topographical analysis was performed on the surface of each membrane via atomic force microscopy (AFM) (Figure 5a-d). First, tapping mode phase images were obtained from each membrane. In these images, the bright region corresponds to the hydrophobic phases of the membrane, while the dark region represents the hydrophilic phases of the membrane. In Nafion-212, distinct phase separation between its hydrophobic PTFE backbone chain and the side chains of the sulfonic acid groups was observed. In contrast, in N-PDA, which contained aromatic dopamine units that were more hydrophobic, a hydrophobic region (the yellowish part) was more pronounced. In N-P(DA-SDA) and N-PSDA with the SDA-containing fillers applied, the higher the SDA content, the more pronounced the well-connected hydrophilic channels, that is, N-P(DA-SDA) < N-PSDA. This was attributed to the introduction of flexible alkyl chains containing sulfonic acid groups in their catecholamine monomers. The reinforcement of hydrophilic channels observed here was also consistent with the WU results described above (Table 1).

The morphology of the Nafion composite membranes was further examined using TEM (Figure 5a'-d'). Nafion is known to form a unique rod-like morphology resulting from phase separation between the backbone hydrophobic perfluorinated polymer chains and the sulfonic acid groups present in its side chains.[45] Accordingly, distinct phase separation between hydrophilic and hydrophobic regions was observed as in the AFM results described above. Ion clusters were found in all tested membranes, formed by the hydrophilic sulfonic acid groups present in the side chains of Nafion. However, in the polydopamine-filled Nafion composite membrane (N-PDA) (Figure 5b′), these ion clusters were smaller than those in Nafion-212 (Figure 5a′). This was because the introduction of the PDA fillers into the swollen Nafion membrane led to dense packing. Well-developed ion clusters were observed in the TEM images of N-P(DA-SDA) (Figure 5c′) and N-PSDA (Figure 5d′), unlike in N-PDA. This was attributed to the introduction of the SDA units containing additional hydrophilic sulfonic acid groups, which then formed additional hydrogen bonds and ionic interactions with Nafion. The magnified TEM images showed that ion clusters were more pronounced and well developed in N-PSDA than in Nafion-212 (Figure S11).

https://doi.org/10.1021/acsomega.2c00263
ACS Omega 2022, 7, 12956−12970

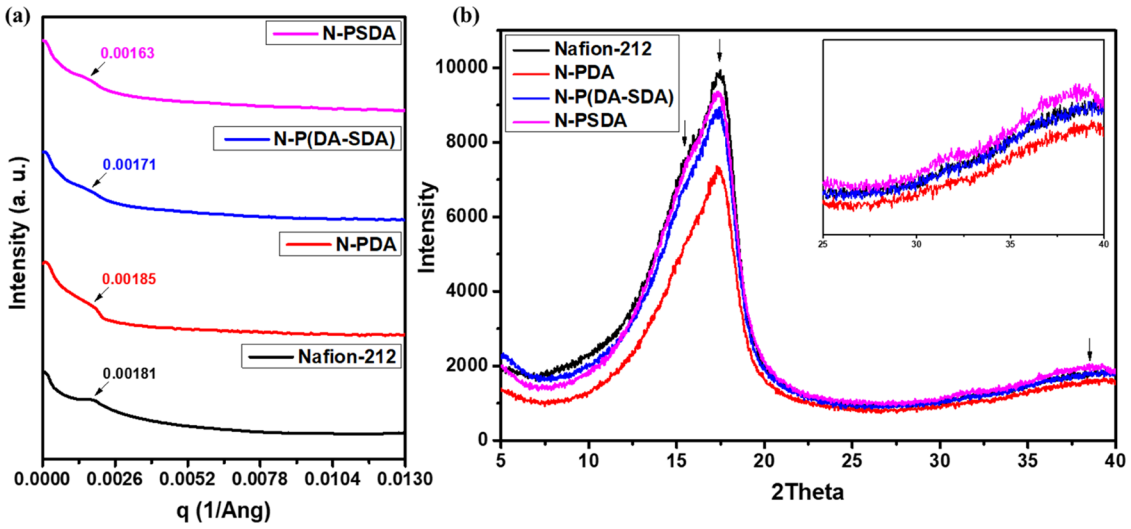

Figure 6. (a) SAXS plots and (b) WAXD plots of the Nafion-212, N-PDA, N-P(DA-SDA), and N-PSDA membranes.

Table 2. Proton Conductivity of the Membranes Filled with Different Polymer Fillers at Different Temperatures

membrane	IEC (meq g^{-1})	proton conductivity (mS cm^{-1})			
	exp	20 °C	40 °C	60 °C	80 °C
Nafion-212	0.91 ± 0.06	95.60 ± 0.21	131.2 ± 0.18	168.8 ± 0.48	204.6 ± 0.72
N-PDA	0.75 ± 0.01	84.4 ± 0.1	113.7 ± 0.3	148.8 ± 0.1	188.7 ± 0.1
N-P(DA-SDA)	0.78 ± 0.01	103.8 ± 0.1	137.7 ± 0.2	177.4 ± 0.3	215.5 ± 0.5
N-PSDA	0.83 ± 0.00	120.9 ± 0.1	160.2 ± 0.3	216.0 ± 0.1	254.3 ± 0.5

The morphology of the Nafion composite membranes was further analyzed using small-angle X-ray scattering (SAXS) and wide-angle X-ray diffraction (WAXD), and the results were compared to those obtained from Nafion-212 (Figure 6).

First, SAXS patterns obtained from the four types of membranes are shown in Figure 6a. Ionomeric peaks of Nafion-212, N-PDA, N-P(DA-SDA), and N-PSDA were observed at q_{max} = 0.00181, 0.00185, 0.00171, and 0.00163 $Å^{-1}$, respectively. Compared with Nafion-212, the ionic cluster size increased (lower q values) for N-P(DA-SDA) and N-PSDA and decreased for N-PDA, indicating that the introduction of PDA fillers into Nafion membranes did not contribute to the formation of large ion clusters, unlike with PSDA. In other words, the dense membrane structure and lack of flexible side chains in the dopamine units caused N-PDA to have the smallest d-spacing (or largest q_{max}). In contrast, N-P(DA-SDA) and N-PSDA exhibited lower q values than Nafion-212, which means their ion domains are larger. This was attributed to the aggregation of sulfonic acid groups contained in the flexible side chains of the SDA units leading to microphase separation while contributing to the formation of proton-conducting channels. These results were also consistent with the AFM (Figure 5a-d) and TEM (Figures 5a'-d' and S11) results, in which an increase in the SDA content enhanced the formation of well-developed hydrophilic ion-conducting channels and ion clusters.

Three characteristic peaks of Nafion were observed in the WAXD patterns of each membrane (Figure 6b). Two scattering peaks were observed in the range of $2\theta \approx 15-20°$: one corresponding to the amorphous region near 16.1° and the other corresponding to the crystalline region near 17.7°. In addition, a diffraction peak attributed to the amorphous packing of Nafion chains was observed near 39°. Similar to those observed in Nafion-212, characteristic peaks corresponding to crystalline and amorphous units were observed in all composite membranes as well.

Changes in the peak corresponding to the amorphous region near 39° were observed in the Nafion composite membranes filled with the PDA derivatives. To be more specific, the degree of crystallinity was higher in N-PDA (2θ = 39.44) than in Nafion-212 (2θ = 38.6). This was due to the PDA filling the pores of the Nafion matrix. Furthermore, the degree of crystallinity decreased with increasing SDA content: 2θ = 39.44, 39.32, and 38.96 for N-PDA, N-P(DA-SDA), and N-PSDA, respectively. This was attributed to the plasticization effect caused by the sulfonic acid groups present in the flexible side chains of the introduced SDA monomers.

3.6. Proton Conductivity of the Membranes. Proton conductivity (σ), an important factor that determines actual cell performance, is significantly affected by the IEC, WU, and morphology of membranes, along with humidity and temperature conditions. The conductivity of the fabricated Nafion composite membranes was measured in water in the temperature range of 20−80 °C (Table 2).

In these conductivity tests, the time required for polymer fillers to completely fill the pores of Nafion membranes during composite membrane fabrication was considered, as presented earlier in the density measurement results (Table S2). Thus, each conductivity measurement was performed at an interval of 12 h. After 36 h, the conductivity remained constant over time at each temperature (Table S6).

In all fabricated membranes, the ionic conductivity increased with the increase in the temperature due to the increased ion mobility caused by thermal activation. In general, ion-conducting polymers with higher IEC values (or higher WU) tend to provide higher ionic conductivity. Accordingly, as

https://doi.org/10.1021/acsomega.2c00263
ACS Omega 2022, 7, 12956−12970

described earlier in the IEC and WU results (Table 1), N-PDA exhibited a lower IEC (0.75 meq g^{-1}) than Nafion-212 at 0.91 meq g^{-1} with a densely packed structure. Thus, the ionic conductivity was lower over the entire temperature range in N-PDA than in Nafion-212 (Table 2).

Meanwhile, polydopamine allows for additional ion transport based on the Grotthuss mechanism in which protons hop from one hydrogen bond site to another. In these membranes, the additional hydrogen bonds the dopamine molecules formed with the sulfonic acid groups of Nafion could also serve the Grotthuss mechanism.[32] It was, therefore, originally expected that N-PDA would exhibit higher ionic conductivity than Nafion-212. However, the ionic conductivity of N-PDA was lower. This was attributed to the fact that filling the high-porosity Nafion matrix with PDA limited ionic conduction via the vehicular mechanism, in which protons are conducted through ion diffusion.

N-P(DA-SDA) and N-PSDA exhibited improved ionic conductivity over the entire temperature range. This was a result of the introduction of flexible alkyl chains containing sulfonic acid groups in their catecholamine monomers. This modification improved the WU (Table 1) and water holding capacity (Figure S10) of the corresponding membranes. Overall, introducing these hydrophilic fillers enhanced the formation of well-developed hydrophilic channels, thereby facilitating ionic conduction. More specifically, N-P(DA-SDA) and N-PSDA were fabricated by filling the pores of Nafion membranes with the sulfonated-PDA fillers with larger free volume (FFV: PDA < P(DA-SDA) < PSDA) (Table S3). In the process, the decrease in ionic conduction via vehicle-type transfer was minimized; at the same time, additional ionic conduction was allowed via the Grotthuss mechanism enabled by the sulfonic acid groups. These results were also consistent with the AFM and TEM (Figure 5) results, in which an increase in the SDA content enhanced the formation of well-developed hydrophilic ion-conducting channels and ion clusters, as shown in the SAXS data (Figure 6a): that is, q_{max} Nafion-212 = 0.00181 $Å^{-1}$ and q_{max} N-PSDA = 0.00163 $Å^{-1}$.

In addition, the activation energy was calculated based on the slopes of the obtained Arrhenius plot (Figure 7). The activation energy of Nafion-212 as the control group was measured as 10.54 kJ mol^{-1}; this is slightly lower than that of N-PDA (11.15 kJ mol^{-1}). Meanwhile, the composite membranes with SDA units exhibited lower activation energy than Nafion-212. This confirmed the contribution of the sulfonic acid groups contained in the SDA units to the formation of additional ion-conducting channels while improving the overall conductivity.

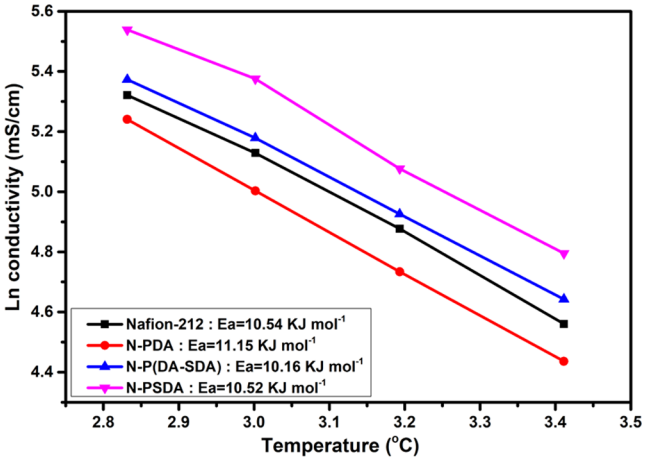

Figure 7. Arrhenius plots of the proton conductivity versus temperature for the membranes with different polymer fillers.

As mentioned earlier, proton conduction requires water molecules to facilitate the transfer process. Thus, ionic conductivity depends significantly on ambient humidity. In the present study, the ionic conductivity of each membrane was measured in the actual operating conditions of fuel cells, that is, at 95% RH and 80 °C (Table S7). The results showed the same patterns as observed in the ionic conductivity results measured in water described above (Table 2). Simply put, N-PDA exhibited significantly lower ionic conductivity than Nafion-212; however, the introduction of the SDA fillers significantly enhanced the ionic conductivity of the corresponding membranes. In particular, the ionic conductivity of N-PSDA was 95.2 mS cm^{-1}, about 23.9% higher than that of Nafion-212, which was 76.8 mS cm^{-1}. This implied that the introduction of SDA and the subsequent formation of hydrophilic ion-conducting channels provided an effective contribution even under high-RH conditions. Overall, in both water and under high-RH conditions, the N-P(DA-SDA) and N-PSDA composite membranes exhibited significantly improved ionic conductivity. Based on the results, these membranes were also expected to provide excellent performance when applied to actual PEMFCs and PEMWE cells.

3.7. Oxidative and Hydrolytic Stability of the Membranes. Next, the oxidative stability of the Nafion composite membranes was examined. The oxidative stability of PEMs is an important parameter that is closely related to the resultant cell performance and durability. Peroxide radicals generated during cell operation may attack the polymer chains of the membrane and chemically degrade the membrane, thereby possibly reducing the overall cell performance.

Each membrane was immersed in Fenton's reagent (4 ppm $FeSO_4$ and 3 wt % H_2O_2) at 80 °C for 6 h. Changes in the weight of each membrane were then measured to examine their ex-situ oxidative stability (Figure S12). The weight retention was about 3.6% higher in Nafion-212 than in N-PDA. N-P(DA-SDA) and N-PSDA exhibited higher oxidative stability than N-PDA, and the degree of improvement increased with increasing SDA content. This was because the sulfonic acid groups attached to the side chains of the SDA units formed strong ionic interactions with the sulfonic acid groups contained in Nafion. In addition, the aliphatic side chains of the SDA units helped keep the aromatic backbone of the PDA fillers in a hydrophobic environment. Note that N-PSDA (96.6%) exhibited a level of oxidative stability comparable to Nafion-212 (98.4%). Given that aromatic hydrocarbon-based polymers with hydrophilic functional groups have relatively low oxidative stability in contrast to Nafion, which is inherently stable due to the C−F bonds in its structure,[46] this result is highly encouraging.

Furthermore, the weight loss was analyzed using TGA for each membrane after treating the membranes with Fenton's reagent (4 ppm $FeSO_4$ and 3 wt % H_2O_2) at 80 °C for 6 h (Figure S13). All of the tested membranes exhibited thermal behavior similar to that of the membranes prior to Fenton's treatment. However, a minute change was observed for N-P(DA-SDA) and N-PSDA at the temperature ranges 280−400 °C (degradation of sulfonic acid groups) and 400−500 °C (degradation of the alkyl side chains of the SDA units),

https://doi.org/10.1021/acsomega.2c00263
ACS Omega 2022, 7, 12956−12970

indicating that the sulfonic acid group degradation occurred not only from the Nafion side chains but also by the alkyl side chains of the SDA units in the sulfonated dopamine-based polymers. Moreover, from the DTG graph, the degradation of the alkyl side chains of SDA units in N-P(DA-SDA) seemed slightly higher compared to N-PSDA; this is in line with the weight loss data shown in Figure S12.

In addition, the remaining conductivity was measured after the oxidative stability test under the same conditions (Figure S14). All of the membranes retained >95% conductivity after this test. While the Nafion-212 membrane showed the lowest weight loss, it suffered from the highest conductivity loss. Meanwhile, the other three composite membranes retained comparatively higher conductivity with increasing SDA content even after Fenton's test; this result is in line with the data in Figure S12. The highest conductivity retention being obtained for N-P(DA-SDA) and N-PSDA suggests that the number of sulfonic acid groups that degraded from the filler polymers is negligible and also shows enhanced oxidative stability.

Following the oxidative stability test, we further analyzed the mechanical properties of the membranes by measuring the stress−strain curves and compared them with those obtained prior to the stability test (Figure S15). The membranes' mechanical properties were found to be affected by Fenton's treatment to a certain extent. Nevertheless, the curves obtained after the stability test exhibited a trend similar to that of the membranes prior to the test (as shown in Figure 3), with similar tensile strength values and relatively lower elongation at break values. Compared to Nafion-212 (tensile stress of 14.3 MPa), the N-PDA (17.8 MPa), N-P(DA-SDA) (17.5 MPa), and N-PSDA (18.5 MPa) membranes retained their tensile strength, indicating that the filler molecules inside the Nafion membrane are nearly stable against the peroxide attack. Notably, the dopamine-based filler molecules can help maintain the membranes' mechanical properties by serving hydrogen bonds and electrostatic interactions with the sulfonic acid functional groups of Nafion. However, the decrease in elongation at break values for the membranes may be caused by the morphological changes resulting from the weight loss during the oxidative stability test. The elongation at break values for Nafion-212, N-PDA, N-P(DA-SDA), and N-PSDA were 180.2, 188.8, 196.6, and 228.2, respectively. Essentially, the composite membranes were also successful in maintaining their tensile strain values. In short, the mechanical properties after the oxidative stability test show that all three composite membranes are efficient in maintaining the mechanical stability required for PEM applications.

Next, durability tests were conducted to assess whether the polydopamine-based fillers might leak from the Nafion membranes. To this end, each composite membrane was immersed in water at 60 °C for 500 h. In the process, changes in conductivity over time were monitored to determine their hydrolytic stability (Figure S16). The hydrolytic stability test results showed that all of the membranes retained >90% conductivity after the long-term durability test in water. More specifically, N-PSDA (100%) exhibited higher hydrolytic stability than the reference Nafion-212 membrane (91.2%) and N-PDA (92.4%). The introduction of sulfonic acid groups significantly enhanced the interaction between the modified filler molecules and the Nafion matrix. This result indicated that the well-connected hydrophilic channels formed as a result of the reaction between the micropores of the Nafion matrix, and the impregnated fillers remained highly stable in water at 60 °C for 500 h.

3.8. Hydrogen Permeability of the Membranes. Subsequently, the hydrogen permeability of the Nafion composite membranes was measured at 60 °C in three conditions: at 5% RH (dry state) and 95% RH, and in water. The results were then compared to those obtained from Nafion-212 (Figure 8 and Table S8). All composite membranes exhibited lower hydrogen permeability than Nafion-212 in all tested conditions, as expected. The hydrogen permeability of N-PDA, in particular, was significantly lower than that of Nafion-212. This was attributed to the fact that the nanopores of Nafion had been filled with the aromatic hydrocarbon-based dopamine units. In addition, the PDA fillers contributed to the narrowing of mass transport channels, that is, hydrogen transport pathways, through the formation of electrostatic attractions and hydrogen bonds with Nafion at the interface between the nanopores and the Nafion matrix. These results confirm that the polymer-filling approach proposed in the present study effectively suppresses hydrogen permeation.

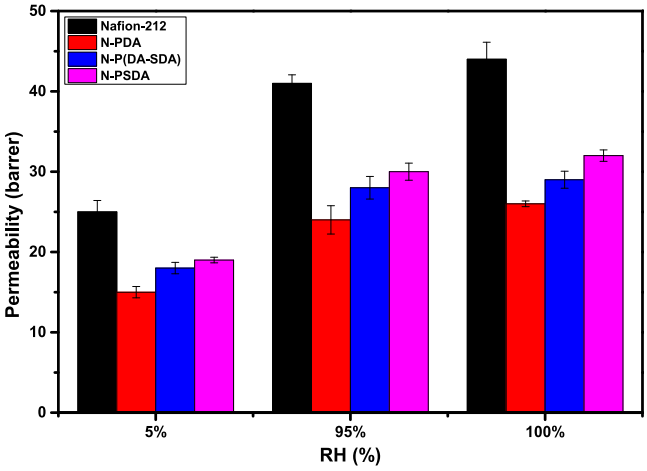

Figure 8. Humidity dependence of hydrogen permeability of Nafion-212, N-PDA, N-P(DA-SDA), and N-PSDA.

The measured hydrogen permeability increased in the order of N-PDA < N-P(DA-SDA) < N-PSDA. This was attributed to the fact that P(DA-SDA) and PSDA had a larger FFV than PDA because their fillers contained sulfonic acid groups in the form of flexible side chains; thus, these polymer fillers were able to increase the free volume of the composite membrane. This tendency was also consistent with those found in the density measurement (Table S2) and crystallinity analysis (Figure 6b) results described above. These results confirm that the increased degree of crystallinity makes composite membranes more resistant to hydrogen permeation.[47] The hydrogen permeability of N-PSDA, in particular, was 26.8% lower at 95% RH (fuel cell operating conditions) and 27.3% lower in a fully hydrated state (water electrolysis operating conditions) than Nafion-212. These results confirm that N-PSDA not only allows ion-conducting channels to be effectively formed but also, at the same time, distorts hydrogen flow passages, thereby significantly reducing hydrogen permeation. When applied to PEMWEs and PEMWE cells, this composite membrane is expected to help control hydrogen crossover in the actual operating conditions of these cells.

https://doi.org/10.1021/acsomega.2c00263
ACS Omega 2022, 7, 12956−12970

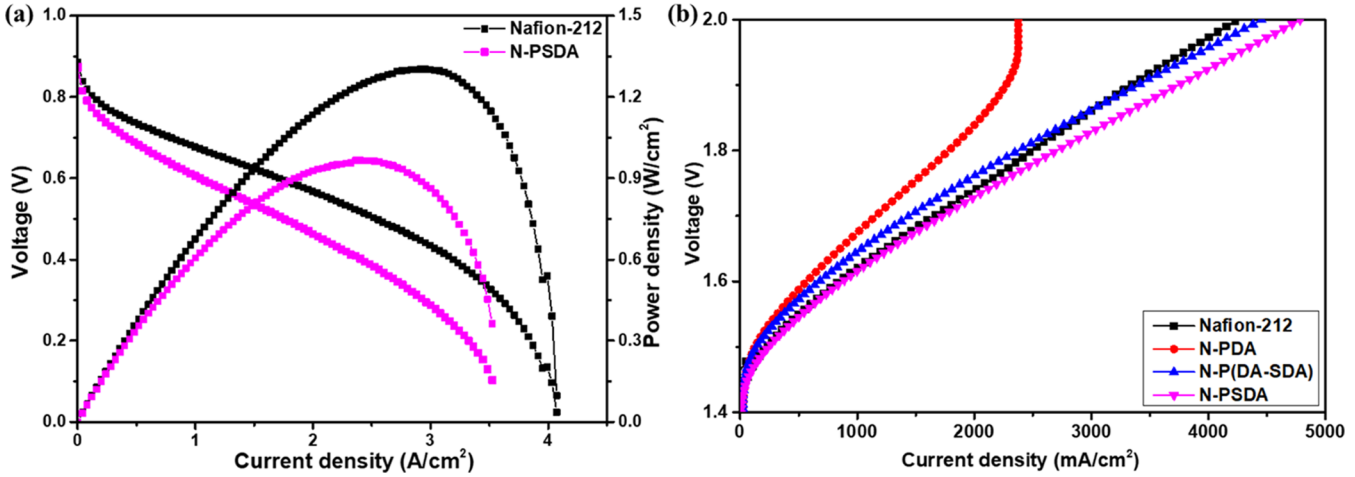

Figure 9. Cell polarization curves of the (a) PEMFC made of Nafion-212 and N-PSDA for H_2/O_2 PEMFC at 80 °C and 100% RH and (b) PEMWEs made of Nafion-212, N-PDA, N-P(DA-SDA), and N-PSDA at 80 °C and 1.6 V.

3.9. Performance of PEM-Based Fuel Cells: PEMFC and PEMWE. Among the fabricated composite membranes, N-PSDA exhibited the best electrochemical and mechanical properties; the membrane was then subjected to single-cell tests at 80 °C and 100% RH, and in H_2 (150 ccm) and O_2 (300 ccm) conditions to determine its cell performance when applied to hydrogen fuel cells. The results were compared to the cell data obtained from pristine Nafion-212 (Figure 9a). The tested membranes were fabricated to have a similar thickness, and the same membrane−electrode assembly (MEA) fabrication procedures were applied to minimize the effect of parameters other than those related to the intrinsic characteristics of the two membranes.

A significant improvement in the cell performance for N-PSDA was expected due to its higher ionic conductivity than pristine Nafion-212. However, in reality, the N-PSDA composite membrane showed worse performance than Nafion-212 under the actual PEMFC operating conditions. The peak power density of the N-PSDA membrane was measured to be 966 mW cm^{-2}, whereas that of Nafion-212 was 1300 mW cm^{-2}. When the applied voltage was 0.6 V, the current density of Nafion-212 was 1690 mA cm^{-2}, whereas N-PDSA showed 1041 mA cm^{-2}. This performance degradation may be related to the interfacial interaction between the membrane and the electrodes, as the MEA performance was greatly influenced by the membrane−electrode interface. In addition, the incompatibility between the hydrocarbon-based electrolyte membrane and the Nafion ionomers can also be a reason for the performance loss of N-PSDA even if the membrane showed higher proton conductivity and lower hydrogen permeability.

Next, the performance of N-PSDA and Nafion-212 as proton exchange membrane water electrolyzers (PEMWEs) was examined. To this end, the single-cell performance of Nafion-212 and N-PSDA was measured in the voltage range of 0−2 V. The results are presented as polarization curves (Figure 9b and Table S9). The N-PSDA membrane exhibited higher cell performance (current density) than Nafion-212. At 2.0 V and 80 °C, in particular, the current density of N-PSDA was 4785 mA cm^{-2}, about 12.5% higher than that of Nafion-212, at 4254 mA cm^{-2}. The high cell performance of the N-PSDA membrane has motivated analysis of the cell performance of N-PDA and N-P(DA-SDA), which achieved current densities of 2376 and 4455 mA cm^{-2}, respectively.

Both N-P(DA-SDA) and N-PSDA showed higher performance than the pristine Nafion-212 membrane. The membranes were also tested for their applicability to PEMWEs at high temperature and at a different voltage level of 1.6 V, i.e., at voltage levels above the thermoneutral voltage of PEMWE at 1.48 V[48,49] (EIS graphs in Figure S17 and Table S10). The results showed that N-PSDA exhibited lower Ohmic resistance than N-P(DA-SDA) and N-PDA. This was attributed to the improved water holding capacity and ionic conductivity of N-PSDA achieved by the introduction of PSDA. In addition, N-P(DA-SDA) followed N-PSDA in performance, thanks to the presence of SDA units that contribute to higher ionic conductivity. Moreover, given that water electrolyzer cells operate in a fully hydrated state, the hydrogen crossover has a greater effect on the cell performance in water electrolyzer cells than in fuel cells operated under RH conditions. Herein, the lower hydrogen permeability of N-P(DA-SDA) and N-PSDA might also be another reason for the higher cell performance, when the N-PDA was an exception due to its lower conductivity.

PFSA membranes are known to exhibit high hydrogen crossover at high temperatures and in hydrated conditions, which reduces the efficiency of hydrogen production in PEMWEs. Hydrogen permeation can be reduced by thickening the membrane, but this increases its Ohmic resistance.[50,51] The hydrogen permeability of membranes with the same thickness was measured and discussed above (Figure 8); in a hydrated state, the hydrogen permeability of Nafion-212 was very high, at 44%, while the figure was lower for N-PSDA, at 32%. Given that the overall performance of PEMWEs significantly depends on the performance of the applied membrane, this decrease in hydrogen crossover observed in N-PSDA was expected to improve the cell performance, especially in high-temperature conditions (80 °C). This can be accounted for as follows: the micropores of Nafion were filled with the PSDA fillers via the in situ SF method, and this modification effectively enhanced the formation of well-developed ion-conducting channels while significantly reducing hydrogen crossover at the membrane−electrode interface and inside the membrane matrix without changing the membrane thickness.

https://doi.org/10.1021/acsomega.2c00263
ACS Omega 2022, 7, 12956−12970

4. CONCLUSIONS

In the present study, sulfonated dopamine was synthesized, and different polymer impregnation agents—PDA, P(DA-SDA), and PSDA—were prepared via the self-oxidation reaction of dopamine. Nafion-212 membranes were impregnated with these agents to fabricate a series of Nafion composite membranes. The prepared polydopamine derivatives filled the nanopores generated in the Nafion framework using the swelling−filling method.

The fractional free volume (FFV) of each polymer was measured, and the degree of filling of the Nafion membranes was analyzed. FT IR analysis and SEM-EDS mapping were performed to confirm the uniform distribution of polydopamine-derivative fillers in the Nafion membrane.

The impregnation agents' catecholamine structure induced strong interactions between the fillers and Nafion matrix, giving the resultant composite membranes improved thermal and mechanical stability compared to Nafion-212 while preventing inhomogeneous phase separation.

Using AFM, SAXS, and TEM, a comprehensive morphological analysis was performed to confirm that, with the introduction of PSDA-containing fillers, the sulfonic acid groups in PSDA side chains allowed further interactions between the Nafion matrix and PSDA fillers, increasing the water uptake of the resultant composite membranes while contributing to the expansion of hydrophilic regions and ion clusters. N-PSDA, which contains well-connected hydrophilic channels, exhibited the highest ionic conductivity. Hydrolytic stability tests confirmed that the membrane could effectively retain its ionic conductivity for 500 h.

Each composite membrane underwent XRD analysis. Filling the nanopores in the Nafion matrix with the polymer fillers containing aromatic hydrocarbon-based dopamine units increased the degree of crystallinity in all tested composite membranes. Consequently, the hydrogen permeability of each composite membrane decreased significantly under both RH and hydrated conditions compared to Nafion-212.

This study is the first to use polydopamine-derivative fillers as impregnation agents for Nafion-212. N-PSDA exhibited a peak power density of 966 mW cm^{-2} and a current density of 4785 mA cm^{-2} when applied to a PEMFC and PEMWE, respectively; the latter is 12.4% higher than Nafion-212 at 2.0 V and 80 °C. These results confirm that N-PSDA enhances the formation of well-developed ion-conducting channels, thus improving the overall cell performance while providing effective control over the hydrogen crossover at the membrane−electrode interface and inside the membrane matrix. Therefore, this material may garner significant attention as a novel material for PEMs in the future.

■ ASSOCIATED CONTENT

Supporting Information

The Supporting Information is available free of charge at https://pubs.acs.org/doi/10.1021/acsomega.2c00263.

Details of additional characterization, synthetic procedure, membrane properties, and measurements data; synthesizing sulfonated dopamine (SDA), ^{1}H NMR and FTIR spectra for SDA; digital photographs of polymer solutions of PDA, P(DA-SDA), and PSDA; UV−vis spectra, SEM surface images, and EDS mapping imaging; FTIR spectra for PDA, P(DA-SDA), and PSDA; digital photographs of composite membranes N-PDA, N-P(DA-SDA), and N-PSDA; FTIR spectra of composite membranes; SEM surface images, DSC analysis, and water state analysis of composite membranes; magnified TEM images Nafion-212 and N-PSDA, oxidative stability, and hydrolytic stability of N-PDA, N-P(DA-SDA), and N-PSDA membranes; EIS curves from PEMWE measurement; table of elemental analysis, density changes, and fractional free volume of PDA, P(DA-SDA), and PSDA polymers; cross-sectional elemental analysis, tensile strength, elongation at break and Young's modulus of composite membranes; time-dependent conductivity, RH conductivity, hydrogen permeability of composite membranes, and current density data obtained from the Nafion-212 and N-PSDA-based PEMWE cell performance; and Ohmic resistance data obtained from the EIS curves (PDF)

■ AUTHOR INFORMATION

Corresponding Author

Tae-Hyun Kim − *Organic Material Synthesis Laboratory, Department of Chemistry, Incheon National University, Incheon 22012, Republic of Korea; Research Institute of Basic Sciences, Incheon National University, Incheon 22012, Republic of Korea;* orcid.org/0000-0002-1654-3785; Phone: +82-32-835-8232; Email: tkim@inu.ac.kr; Fax: +82-32-835-0762

Authors

T. S. Mayadevi − *Organic Material Synthesis Laboratory, Department of Chemistry, Incheon National University, Incheon 22012, Republic of Korea; Research Institute of Basic Sciences, Incheon National University, Incheon 22012, Republic of Korea*

Bon-Hyuk Goo − *Organic Material Synthesis Laboratory, Department of Chemistry, Incheon National University, Incheon 22012, Republic of Korea; Research Institute of Basic Sciences, Incheon National University, Incheon 22012, Republic of Korea*

Sae Yane Paek − *Hydrogen and Fuel Cell Research Center, Korea Institute of Science and Technology (KIST), Seoul 02792, Republic of Korea*

Ook Choi − *Research Institute of Basic Sciences, Incheon National University, Incheon 22012, Republic of Korea*

Youngkwang Kim − *School of Chemical and Biological Engineering, Seoul National University, Seoul 08826, Republic of Korea;* orcid.org/0000-0002-1843-366X

Oh Joong Kwon − *Department of Energy and Chemical Engineering and Innovation Center for Chemical Engineering, Incheon National University, Incheon 22012, Republic of Korea;* orcid.org/0000-0002-7745-433X

So Young Lee − *Hydrogen and Fuel Cell Research Center, Korea Institute of Science and Technology (KIST), Seoul 02792, Republic of Korea*

Hyoung-Juhn Kim − *Hydrogen and Fuel Cell Research Center, Korea Institute of Science and Technology (KIST), Seoul 02792, Republic of Korea; Hydrogen Energy Technology Laboratory, Korea Institute of Energy Technology (KENTECH), Naju-si, Jeollanam-do 58217, Republic of Korea*

Complete contact information is available at: https://pubs.acs.org/10.1021/acsomega.2c00263

https://doi.org/10.1021/acsomega.2c00263
ACS Omega 2022, 7, 12956−12970

Author Contributions

○M.T.S. and B.-H.G. contributed equally to this work. The manuscript was written through contributions of all authors. All authors have given approval to the final version of the manuscript.

Notes

The authors declare no competing financial interest.

■ ACKNOWLEDGMENTS

This work was supported by a grant from the National Research Foundation of Korea (NRF) funded by the Ministry of Education (2021M1A2A2038114). Part of this work was also supported by Incheon National University Research Grant in 2020.

■ REFERENCES

(1) Haider, R.; Wen, Y.; Ma, Z. F.; Wilkinson, D. P.; Zhang, L.; Yuan, X.; Song, S.; Zhang, J. High Temperature Proton Exchange Membrane Fuel Cells: Progress in Advanced Materials and Key Technologies. *Chem. Soc. Rev.* **2021**, *50*, 1138−1187.

(2) Ogungbemi, E.; Wilberforce, T.; Ijaodola, O.; Thompson, J.; Olabi, A. G. Selection of Proton Exchange Membrane Fuel Cell for Transportation. *Int. J. Hydrogen Energy* **2021**, *46*, 30625−30640.

(3) Alaswad, A.; Omran, A.; Sodre, J. R.; Wilberforce, T.; Pignatelli, G.; Dassisti, M.; Baroutaji, A.; Olabi, A. G. Technical and Commercial Challenges of Proton-Exchange Membrane (PEM) Fuel Cells. *Energies* **2020**, *14*, No. 144.

(4) Lindquist, G. A.; Xu, Q.; Oener, S. Z.; Boettcher, S. W. Membrane Electrolyzers for Impure-Water Splitting. *Joule* **2020**, *4*, 2549−2561.

(5) Shirvanian, P.; van Berkel, F. Novel Components in Proton Exchange Membrane (PEM) Water Electrolyzers (PEMWE): Status, Challenges and Future Needs. A Mini Review. *Electrochem. Commun.* **2020**, *114*, 106704−106707.

(6) Yodwong, B.; Guilbert, D.; Phattanasak, M.; Kaewmanee, W.; Hinaje, M.; Vitale, G. Proton Exchange Membrane Electrolyzer Modeling for Power Electronics Control: A Short Review. *C* **2020**, *6*, 29−48.

(7) Okonkwo, P. C.; Ben Belgacem, I.; Emori, W.; Uzoma, P. C. Nafion Degradation Mechanisms in Proton Exchange Membrane Fuel Cell (PEMFC) System: A Review. *Int. J. Hydrogen Energy* **2021**, *46*, 27956−27973.

(8) Passalacqua, E.; Pedicini, R.; Carbone, A.; Gatto, I.; Matera, F.; Patti, A.; Saccà, A. Effects of the Chemical Treatment on the Physical-Chemical and Electrochemical Properties of the Commercial Nafion NR212 Membrane. *Materials* **2020**, *13*, 5254−5269.

(9) Xu, G.; Li, J.; Ma, L.; Xiong, J.; Mansoor, M.; Cai, W.; Cheng, H. Performance Dependence of Swelling-Filling Treated Nafion Membrane on Nano-Structure of Macromolecular Filler. *J. Membr. Sci.* **2017**, *534*, 68−72.

(10) Xing, Y.; Li, H.; Avgouropoulos, G. Research Progress of Proton Exchange Membrane Failure and Mitigation Strategies. *Materials* **2021**, *14*, 2591−2607.

(11) Vinothkannan, M.; Ramakrishnan, S.; Kim, A. R.; Lee, H. K.; Yoo, D. J. Ceria Stabilized by Titanium Carbide as a Sustainable Filler in the Nafion Matrix Improves the Mechanical Integrity, Electrochemical Durability, and Hydrogen Impermeability of Proton-Exchange Membrane Fuel Cells: Effects of the Filler Content. *ACS Appl. Mater. Interfaces* **2020**, *12*, 5704−5716.

(12) Oh, K.; Kwon, O.; Son, B.; Lee, D. H.; Shanmugam, S. Nafion-Sulfonated Silica Composite Membrane for Proton Exchange Membrane Fuel Cells under Operating Low Humidity Condition. *J. Membr. Sci.* **2019**, *583*, 103−109.

(13) Feng, K.; Tang, B.; Wu, P. Sulfonated Graphene Oxide-Silica for Highly Selective Nafion-Based Proton Exchange Membranes. *J. Mater. Chem. A* **2014**, *2*, 16083−16092.

(14) Vinothkannan, M.; Hariprasad, R.; Ramakrishnan, S.; Kim, A. R.; Yoo, D. J. Potential Bifunctional Filler (CeO_2-ACNTs) for Nafion Matrix toward Extended Electrochemical Power Density and Durability in Proton-Exchange Membrane Fuel Cells Operating at Reduced Relative Humidity. *ACS Sustainable Chem. Eng.* **2019**, *7*, 12847−12857.

(15) S, R. R. R.; Rashmi, W.; Khalid, M.; Wong, W. Y.; Priyanka, J. Recent Progress in the Development of Aromatic Polymer-Based Proton Exchange Membranes for Fuel Cell Applications. *Polymers* **2020**, *12*, 1061−1087.

(16) Mohammadi, M.; Mehdipour-Ataei, S. Durable Sulfonated Partially Fluorinated Polysulfones as Membrane for PEM Fuel Cell. *Renewable Energy* **2020**, *158*, 421−430.

(17) Lee, K. H.; Chu, J. Y.; Mohanraj, V.; Kim, A. R.; Song, M. H.; Yoo, D. J. Enhanced Ion Conductivity of Sulfonated Poly(Arylene Ether Sulfone) Block Copolymers Linked by Aliphatic Chains Constructing Wide-Range Ion Cluster for Proton Conducting Electrolytes. *Int. J. Hydrogen Energy* **2020**, *45*, 29297−29307.

(18) Miyake, J.; Kusakabe, M.; Tsutsumida, A.; Miyatake, K. Remarkable Reinforcement Effect in Sulfonated Aromatic Polymers as Fuel Cell Membrane. *ACS Appl. Energy Mater.* **2018**, *1*, 1233−1238.

(19) Li, J.; Bu, F.; Ru, C.; Jiang, H.; Duan, Y.; Sun, Y.; Pu, X.; Shang, L.; Li, X.; Zhao, C. Enhancing the Selectivity of Nafion Membrane by Incorporating a Novel Functional Skeleton Molecule to Improve the Performance of Direct Methanol Fuel Cells. *J. Mater. Chem. A* **2020**, *8*, 196−206.

(20) Li, J.; Fan, K.; Cai, W.; Ma, L.; Xu, G.; Xu, S.; Ma, L.; Cheng, H. An In-Situ Nano-Scale Swelling-Filling Strategy to Improve Overall Performance of Nafion Membrane for Direct Methanol Fuel Cell Application. *J. Power Sources* **2016**, *332*, 37−41.

(21) Li, J.; Xu, G.; Luo, X.; Xiong, J.; Liu, Z.; Cai, W. Effect of Nano-Size of Functionalized Silica on Overall Performance of Swelling-Filling Modified Nafion Membrane for Direct Methanol Fuel Cell Application. *Appl. Energy* **2018**, *213*, 408−414.

(22) Xu, G.; Wu, Z.; Wei, Z.; Zhang, W.; Wu, J.; Li, Y.; Li, J.; Qu, K.; Cai, W. Non-Destructive Fabrication of Nafion/Silica Composite Membrane via Swelling-Filling Modification Strategy for High Temperature and Low Humidity PEM Fuel Cell. *Renewable Energy* **2020**, *153*, 935−939.

(23) Li, J.; Xu, G.; Cai, W.; Xiong, J.; Ma, L.; Yang, Z.; Huang, Y.; Cheng, H. Non-Destructive Modification on Nafion Membrane via in-Situ Inserting of Sheared Graphene Oxide for Direct Methanol Fuel Cell Applications. *Electrochim. Acta* **2018**, *282*, 362−368.

(24) Xu, G.; Li, J.; Ma, L.; Xiong, J.; Mansoor, M.; Cai, W.; Cheng, H. Performance Dependence of Swelling-Filling Treated Nafion Membrane on Nano-Structure of Macromolecular Filler. *J. Membr. Sci.* **2017**, *534*, 68−72.

(25) Xu, G.; Xue, S.; Wei, Z.; Li, J.; Qu, K.; Li, Y.; Cai, W. Stabilizing Phosphotungstic Acid in Nafion Membrane via Targeted Silica Fixation for High-Temperature Fuel Cell Application. *Int. J. Hydrogen Energy* **2021**, *46*, 4301−4308.

(26) Liu, Y.; Ai, K.; Lu, L. Polydopamine and Its Derivative Materials: Synthesis and Promising Applications in Energy, Environmental, and Biomedical Fields. *Chem. Rev.* **2014**, *114*, 5057−5115.

(27) Hong, S.; You, I.; Song, I. T.; Lee, H. Material-Independent Surface Modification Inspired by Mussel-Adhesion. *Polym. Sci. Technol.* **2015**, *23*, 396−406.

(28) Eom, S.; Key, H.; Jihyo, P.; Seonki, P.; Lee, H. Recent Progress on Polydopamine Surface Chemistry. *Adhes. Interfaces* **2018**, *19*, 19−29.

(29) Yoon, K. R.; Lee, K. A.; Jo, S.; Yook, S. H.; Lee, K. Y.; Kim, I. D.; Kim, J. Y. Mussel-Inspired Polydopamine-Treated Reinforced Composite Membranes with Self-Supported CeO_x Radical Scavengers for Highly Stable PEM Fuel Cells. *Adv. Funct. Mater.* **2019**, *29*, 1806929−1806939.

(30) Liebscher, J. Chemistry of Polydopamine − Scope, Variation, and Limitation. *Eur. J. Org. Chem.* **2019**, *2019*, 4976−4994.

(31) Zhang, H.; Hu, Q.; Zheng, X.; Yin, Y.; Wu, H.; Jiang, Z. Incorporating Phosphoric Acid-Functionalized Polydopamine into

https://doi.org/10.1021/acsomega.2c00263
ACS Omega 2022, 7, 12956−12970

Nafion Polymer by in Situ Sol-Gel Method for Enhanced Proton Conductivity. *J. Membr. Sci.* **2019**, *570-571*, 236−244.
(32) Ram, F.; Velayutham, P.; Sahu, A. K.; Lele, A. K.; Shanmuganathan, K. Enhancing Thermomechanical and Chemical Stability of Polymer Electrolyte Membranes Using Polydopamine Coated Nanocellulose. *ACS Appl. Energy Mater.* **2020**, *3*, 1988−1999.
(33) Ding, J.; Wu, H.; Wu, P. Development of Nanofiltration Membranes Using Mussel-Inspired Sulfonated Dopamine for Interfacial Polymerization. *J. Membr. Sci.* **2020**, *598*, 117658−117667.
(34) Chen, T. P.; Liu, T.; Su, T. L.; Liang, J. Self-Polymerization of Dopamine in Acidic Environments without Oxygen. *Langmuir* **2017**, *33*, 5863−5871.
(35) Mazario, E.; Sánchez-Marcos, J.; Menéndez, N.; Herrasti, P.; García-Hernández, M.; Muñoz-Bonilla, A. One-Pot Electrochemical Synthesis of Polydopamine Coated Magnetite Nanoparticles. *RSC Adv.* **2014**, *4*, 48353−48361.
(36) Liu, T.; Kim, K. C.; Lee, B.; Chen, Z.; Noda, S.; Jang, S. S.; Lee, S. W. Self-Polymerized Dopamine as an Organic Cathode for Li- and Na-Ion Batteries. *Energy Environ. Sci.* **2017**, *10*, 205−215.
(37) Addisu, K. D.; Hailemeskel, B. Z.; Mekuria, S. L.; Andrgie, A. T.; Lin, Y. C.; Tsai, H. C. Bioinspired, Manganese-Chelated Alginate-Polydopamine Nanomaterials for Efficient in Vivo T1-Weighted Magnetic Resonance Imaging. *ACS Appl. Mater. Interfaces* **2018**, *10*, 5147−5160.
(38) Sieuw, L.; Jouhara, A.; Quarez, É.; Auger, C.; Gohy, J. F.; Poizot, P.; Vlad, A. A H-Bond Stabilized Quinone Electrode Material for Li-Organic Batteries: The Strength of Weak Bonds. *Chem. Sci.* **2019**, *10*, 418−426.
(39) Luo, H.; Gu, C.; Zheng, W.; Dai, F.; Wang, X.; Zheng, Z. Facile Synthesis of Novel Size-Controlled Antibacterial Hybrid Spheres Using Silver Nanoparticles Loaded with Poly-Dopamine Spheres. *RSC Adv.* **2015**, *5*, 13470−13477.
(40) Yuan, C.; Liu, Q.; Chen, H.; Huang, A. Mussel-Inspired Polydopamine Modification of Supports for the Facile Synthesis of Zeolite LTA Molecular Sieve Membranes. *RSC Adv.* **2014**, *4*, 41982−41988.
(41) Zhang, P.; Li, W.; Wang, L.; Gong, C.; Ding, J.; Huang, C.; Zhang, X.; Zhang, S.; Wang, L.; Bu, W. Polydopamine-Modified Sulfonated Polyhedral Oligomeric Silsesquioxane: An Appealing Nanofiller to Address the Trade-off between Conductivity and Stabilities for Proton Exchange Membrane. *J. Membr. Sci.* **2020**, *596*, 117734−117723.
(42) Rao, A. S.; Rashmi, K. R.; Manjunatha, D. V.; Jayarama, A.; Prabhu, S.; Pinto, R. Pore Size Tuning of Nafion Membranes by UV Irradiation for Enhanced Proton Conductivity for Fuel Cell Applications. *Int. J. Hydrogen Energy* **2019**, *44*, 23762−23774.
(43) Ru, C.; Gu, Y.; Duan, Y.; Zhao, C.; Na, H. Enhancement in Proton Conductivity and Methanol Resistance of Nafion Membrane Induced by Blending Sulfonated Poly(Arylene Ether Ketones) for Direct Methanol Fuel Cells. *J. Membr. Sci.* **2019**, *573*, 439−447.
(44) Guo, B.; Tay, S. W.; Liu, Z.; Hong, L. Embedding of Hollow Polymer Microspheres with Hydrophilic Shell in Nafion Matrix as Proton and Water Micro-Reservoir. *Polymers* **2012**, *4*, 1499−1516.
(45) Ryu, S.; Kim, J. H.; Lee, J. Y.; Moon, S. H. Investigation of the Effects of Electric Fields on the Nanostructure of Nafion and Its Proton Conductivity. *J. Mater. Chem. A* **2018**, *6*, 20836−20843.
(46) Wang, L. M.; Zhang, Q. F.; Zhang, S. B. A Facile Method for Preparation of Cardo Poly(Aryl Ether Sulfone) Bearing Pendent Sulfoalkyl Groups as Proton Exchange Membranes. *Chin. J. Polym. Sci.* **2015**, *33*, 1225−1233.
(47) Rangel-Cárdenas, A.; Koper, G. Transport in Proton Exchange Membranes for Fuel Cell Applications—A Systematic Non-Equilibrium Approach. *Materials* **2017**, *10*, 576−593.
(48) Scheepers, F.; Stähler, M.; Stähler, A.; Rauls, E.; Müller, M.; Carmo, M.; Lehnert, W. Temperature Optimization for Improving Polymer Electrolyte Membrane-Water Electrolysis System Efficiency. *Appl. Energy* **2021**, *283*, 116270−116280.
(49) Babic, U.; Suermann, M.; Büchi, F. N.; Gubler, L.; Schmidt, T. J. Critical Review—Identifying Critical Gaps for Polymer Electrolyte Water Electrolysis Development. *J. Electrochem. Soc.* **2017**, *164*, F387−F399.
(50) Omrani, R.; Shabani, B. Hydrogen Crossover in Proton Exchange Membrane Electrolysers: The Effect of Current Density, Pressure, Temperature, and Compression. *Electrochim. Acta* **2021**, *377*, 138085−138101.
(51) Schalenbach, M.; Tjarks, G.; Carmo, M.; Lueke, W.; Mueller, M.; Stolten, D. Acidic or Alkaline? Towards a New Perspective on the Efficiency of Water Electrolysis. *J. Electrochem. Soc.* **2016**, *163*, F3197−F3208.

https://doi.org/10.1021/acsomega.2c00263
ACS Omega 2022, 7, 12956−12970